British Journal of Applied Science & Technology
3(3): 609-625, 2013

SCIENCEDOMAIN *international*
www.sciencedomain.org

The Convergence of Normalized Vehicular Rolling Friction Coefficient (C_{rr}) by Dynamic High-Speed Imaging and Least Square Optimization Techniques

Sanwar A. Sunny[1*]

[1]*Department of Mechanical Engineering, University of Kansas, Lawrence, KS 66045, USA.*

Author's contribution

The only author performed the whole research work. Author SAS wrote the first draft of the paper. Author SAS read and approved the final manuscript.

Research Article

Received 7th February 2013
Accepted 4th April 2013
Published 23rd April 2013

ABSTRACT

The paper describes a simple, small scale and low cost yet comprehensive approach to quantifying the Coefficient of Rolling Resistance/Friction (C_{rr}) also known as the Rolling Resistance Coefficient in automobiles. C_{rr} is usually defined as the amount of force required to overcome the hysteresis of the material during tire rotation, where reduced C_{rr} tires can save 1.5–4.5% of automotive fuel consumption. Automotive Standards from the Society of Automotive Engineers use to quantify C_{rr} namely SAE J2452 and SAE J1269 were briefly introduced. Methods of coast down and speed trap tests were conducted under varying body weighted conditions to find the coefficient value, where a high speed camera monitored the motion of the vehicle. The experiment produced different equations of motion which were then solved analytically by numerical analysis techniques to converge on the rolling friction coefficient. A scaled model was used to run dynamic tests and the Reynolds Number (Re) was used to establish a relationship between model and full scale vehicle velocities. Initial guesses in the least square optimization iterations provided coefficient values where drag forces were normalized by assuming constant drag coefficient (C_D of 0.40) and then neglecting its contribution during vehicle motion due to the test model size, resulting in a mean C_{rr} of 0.0116. The study results were compared with 3 studies and also against an automotive C_{rr} model. Schmidt 2010 Dynatest Green Road report shares a high 43% error, while the National Academy of Sciences, 2006 and

**Corresponding author: E-mail: sanwar@ku.edu, sanwarsunny@umkc.edu;*

Gillespie, 1992 yielded errors of 10.5% and 7.2%. The recent mathematical model of Ehsani 2009 yielded an average C_{rr} value error of 2.3% (with individual test averages of 0.80%). Direct scaling and multiplying abilities were attributed for quantifying the normalized value in the study.

Keywords: Coefficient of rolling resistance; curb weight; rolling friction; least square optimization methods; vehicle fuel efficiency; aerodynamic drag coefficient.

1. INTRODUCTION

Vehicle motion is caused by axle rotation which is in turn powered by the combustion in the automobile engine. As the power is cut from the source, the vehicle comes to rest due to internal friction, aerodynamic drag and rolling resistance at the wheels. The external frictional forces at the wheels are directly depended on the total vehicle weight, the traveling velocity and a proportional constant called the coefficient of rolling friction. This constant, denoted in this study as C_{rr}, depends on the texture and structure of the road, vehicle weight and the wheel dimensions, among other factors. Frictional forces caused by air movement over the car are called drag forces [1].

In recent years, the automotive industry has conducted research on finding and minimizing external forces hindering a car's motion. Better tire designs and threading techniques are becoming prevalent design considerations as manufacturers are now shifting focus from performance towards efficiency, striving to power more engine energy to the wheels and incurring lesser losses in the process. Almost always a dynamic testing approach is necessary for converging on the rolling friction coefficient. Coast down testing is a viable experiment conducted universally to observe the effects of rolling friction in moving bodies. In these testing, power from the engine is cut at a certain point, after which mostly external forces work to slow down the body and ultimately bring the body to rest over a certain period of time. This distance and time period is then observed, monitored and numerically treated with fundamental vehicular motion laws of classical mechanics. With known parameters, advanced numerical analysis is then conducted on the results to find pertinent information key to the vehicle's performance. Although overall body mass is a great factor in reducing wheel friction, rolling resistance coefficient can be reduced to optimize a vehicle's performance and fuel efficiency [2]. In recent times, scientists and researchers have begun testing the automobile computationally to find important design parameters. The tests include Computational Fluid Dynamics (CFD) studies for fluid flow around an object [3] such as the vehicle exterior or even modeling and testing exterior panels using Finite Element Analysis (FEA) [4]. Tires can also be constructed and tested to analyze the relationship between wheel design and the coefficient of rolling resistance in FEA with 2D and 3D modeling [5].

The present investigation, however, is to introduce a coast down technique which further utilizes a speed trap system by high speed imaging processes in a dynamic motion by a scaled model. Due to geometric similitude principles, a $1{:}10^{th}$ scale model of a 1974 Model Volkswagen Super beetle will be used. Entry and exit points will be identified at which the vehicle will pass during two different separate points of time, and the time required to cover the distance in between will be numerically computed from video data. The overall body weight will be varied throughout the experiment to generate multiple equation models which will be solved analytically to converge on the constant after utilizing elementary numerical least square optimization techniques. There exists other coast down technique where speed

and deceleration values in tests are effectively eliminated and is based on the time–distance function derived by new solutions of the coast-down equation that is free from speed and deceleration. This enables a considerable group of measurement error sources to be eliminated and the coast-down technique sensitivity to be increased; so the small drag alterations due to the changes in vehicle aerodynamic configuration or tire parameters, such as load, inflation pressure and temperature, can be detected [6].

2. MATERIALS AND METHODS

Asphalt is chosen as the terrain for all the tests to imitate actual driving conditions. A scaled wireless model is used to run the tests. Due to principles of the Reynolds Number (Re) and Similitude, the following assumptions were made to extrapolate to full scale results. To scale the velocities for the car and the model, we use principles of geometric similitude by comparing the Reynolds's number, knowing that:

$\mathrm{Re} = \frac{u\sqrt{A}}{v}$ where u is the velocity, A is the cross-sectional area, D is the diameter, $v = \frac{\mu}{\rho}$ (V is the fluid viscosity, ρ is the fluid density, and μ is the kinematic viscosity). We assume $\sqrt{A} = D$ (in meters), hence the number now becomes $\mathrm{Re} = \frac{\rho u D}{\mu}$, and we can establish the relationship between the model and the full scale car by the respective Reynolds numbers.

$\left[\frac{\rho u D}{\mu}\right]_{scaled} = \left[\frac{\rho u D}{\mu}\right]_{full}$ where the vehicle velocity ratio is given by $u_{scaled} = u_{full} \times \left(\frac{\rho_{full}}{\rho_{scaled}}\right) \times \left(\frac{D_{full}}{D_{scaled}}\right) \times \left(\frac{\mu_{scaled}}{\mu_{full}}\right)$, the densities ρ and kinematic viscosities μ cancel out due to the fluids being the same (air under standard temperature and pressure) or $u_{scaled} = 10 \times u_{full}$; meaning that for the scaled model to experience the same magnitude of drag forces as full scaled vehicle, the speed at which it needs to run in would need to be 10 times the actual car speed. The entrance point (1) and the exit point (2) are spaced 103.5 inches (denoted in calculations as X_{trap}) away from each other. Fig. 1. A 0.333 fps (frames per second) high definition camera was placed at the midpoint of the track to monitor the distances traveled with unit time. X_1 and X_2 refer to the exit first and second locations, while L_2 and L_1 refer to the entrance first and second locations respectively. SC_{ent} and SC_{ex} were manually computed and dimensionless scaling coefficients incorporated in the expressions to account for the discrepancies in measurements due to the spacing of the camera and the running track. Entrance and exit velocities respectively were calculated as $V_{ent} = \frac{dl}{dt} = \frac{L_2 - L_1}{\Delta t_{fps}}$ and $V_{ex} = \frac{dl}{dt} = \frac{X_2 - X_1}{\Delta t_{fps}}$ (where Δt_{fps} = time lapse computed from the camera frames) from where we say the mean velocity, $\overline{V} = \frac{1}{2}\left(V_{ex} + V_{ent}\right)$ from which the

acceleration *a*, or $\frac{\Delta V_0}{\Delta t}$ was numerically computed with ΔV_0 being the initial velocity and Δt being the time required for the car to completely clear the distance. Figs. 2a and b. The average acceleration:

$\bar{a} = \frac{dv}{dt} = \frac{V_{ex} - V_{ent}}{\Delta t}$ (where $\Delta t = \frac{X_{trap}}{\bar{V}}$ and the total track distance is $X_{trap} + X_2 - X_1$ or $X_{trap} + L_2 - L_1$) data was computed and is shown in the results section. This gives us $\mathrm{F}_{\mathrm{Supplied}} = m_t \bar{a}$ (where m_t was varied by adding weights) where deceleration is caused due to drag and rolling resistance and thus $m_t \bar{a}$ can equated to $F_{Drag} + F_{Rolling}$ and also $\mathrm{F}_{\mathrm{Rolling}} = C_{rr} W \bar{V}$ (C_{rr} is the coefficient of rolling resistance; which is depended on wheel and road factors, among other conditions), where the weight $W = m_t g$; a simplified force balance on the vehicle body showed the since $\sum F = 0$, $F_{Supplied} - F_{Drag} - F_{Rolling}$, where $F_{Drag} = \frac{1}{2} C_D \rho_{air} A_{frontal} V^2$. This model is built on the assumption that during coast down, drag and rolling friction forces are all that acts on the car. Another assumption pertaining to automotive drag would be neglecting any headwind or tailwind to the car. To fully quantify $F_{Drag,}$ the drag coefficient C_D for the vehicle needs to be experimentally quantified, and any headwind or tailwind would produce an erroneous coefficient value if they are not added or subtracted from the velocity. Although at speeds traveled by the car during these speed trap tests, drag forces are negligible. In any case, for better convergence on the coefficients of rolling friction, using drag coefficients would eliminate margins of error within the equations of motion (force balance and mechanics equations).

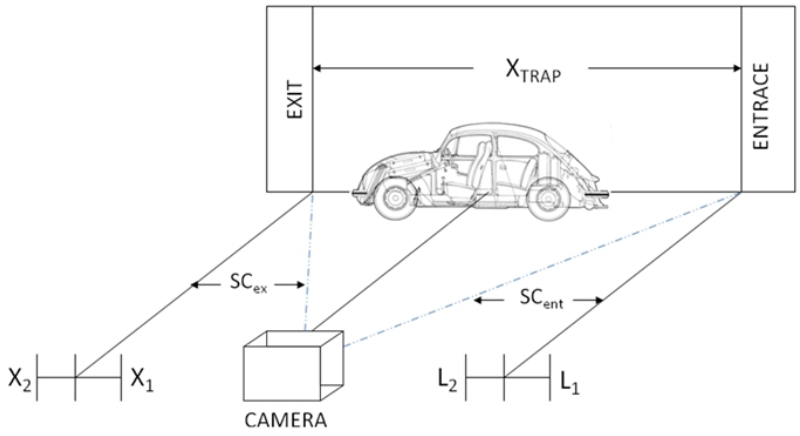

Fig. 1. Experimental setup

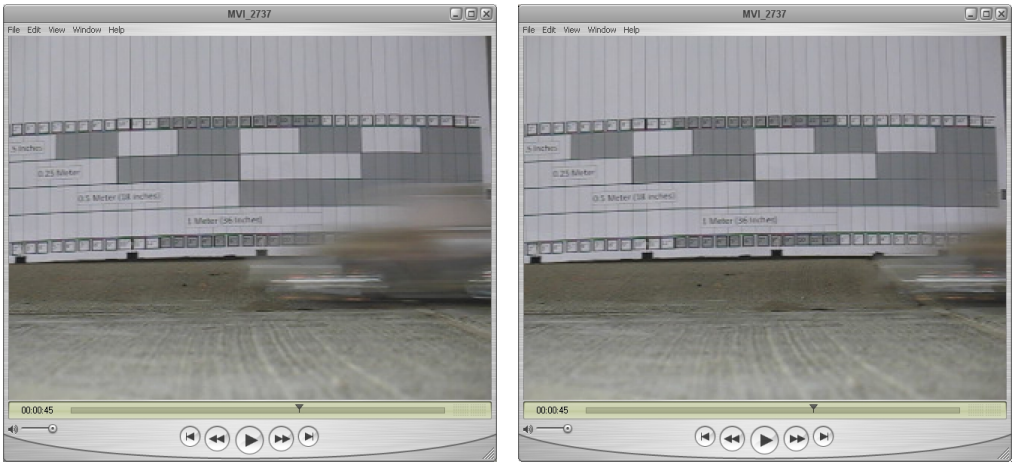

Fig. 2. a-b. Two frames of the camera imaging of dynamic speed trap tests

Drag forces (F_{Drag} or F_D) of a car are depended on C_D, the coefficient of aerodynamic drag for the certain shape, ρ_{air}, the mass density of the fluid through which the body is traveling, $A_{frontal}$ or the vehicle's effective frontal area and most importantly u, the mean velocity of the car. $A_{frontal}$ is calculated both manually through photo pixelization and computationally through taking a section view and measuring the enclosed area in a 3-D CAD software. The value of $A_{frontal}$ was 0.0221 m^2. Moreover, v_o is introduced as the fluid viscosity.

Using the algorithms of the Pi Theorem, theory states that the drag forces which depend on the five above parameters [7]; or $f_x(F_D, u, A_{frontal}, \rho_{air}, v_0) = 0$ can be reduced using two dimensionless parameters, culminating in the Reynolds number, where $\mathrm{Re} = \frac{u\sqrt{A}}{v}$, and the Coefficient of Drag (C_D), where $C_D = \frac{F_D}{\frac{1}{2}\rho_{air} A_{frontal} u^2}$. Hence the function of five variables can be effectively reduced by introducing a function of only two variables; where f_y is some function of two arguments:

$f_y\left(\frac{F_D}{\frac{1}{2}\rho_{air} A_{frontal} u^2}, \frac{u\sqrt{A}}{v}\right) = 0$, which finally yields $F_D = \frac{1}{2} C_D \rho_{air} A_{frontal} u^2$, as noted in [8]. This speed (u) would be noted on the venture meter height readings or H (cm) and the changes in height (Δh) will correspond to changes in velocities u (mph) which in this studies' data analysis will be denoted as a V. Further theory also provides a direct method of establishing a relationship between height readings and wind tunnel air speeds [9]. It is now known universally as the Bernoulli's Principle.

It is suggested that the work-energy theorem can be used to derive Bernoulli's principle $W = \Delta E_k$ i.e the change in the kinetic energy E_k of the system is equal to the net work W done on the system [10]; the system itself consists of a volume of incompressible fluid, between two distinct cross sectional areas given by A_1 and A_2 moving over the distances d_1 and d_2 respectively, where $d_i = v_i \cdot \Delta t$. The displaced fluid volumes are $A_1 d_1$ and $A_2 d_2$; implying that the displaced masses are $\rho A_1 d_1$ and $\rho A_2 d_2$, hence $\rho A_1 d_1 = \rho A_1 v_1 \Delta t = \Delta m$ and $\rho A_2 d_2 = \rho A_2 v_2 \Delta t = \Delta m$ (with ρ being the fluid's mass density, Δt being the time interval through which the masses are displaced and the displaced mass denoted by Δm). The work done by pressure along the areas:

$W_p = F_{p,1}\, d_1 - F_{p,2}\, d_2$ which equals $p_1 A_1 d_1 - p_2 A_2 d_2$ which becomes $\Delta m \frac{p_1}{\rho} - \Delta m \frac{p_2}{\rho}$ the work done mostly by gravity (the gravitational potential energy in the volume $A_1 d_1$ is lost, and at the outflow in the volume $A_2 d_2$ is gained) can be written as $\Delta E_g = \Delta m g z_2 - \Delta m g z_1$ or $W_g = -\Delta E_g = \Delta m g z_1 - \Delta m g z_2$ [11], the total work done in this time interval Δt being $W_t = W_g + W_p$ which means an increase in kinetic energy given by $\Delta E_k = \frac{1}{2}\Delta m u_2^2 - \frac{1}{2}\Delta m u_1^2$. Hence putting all these together, the work-kinetic energy theorem can be rearranged into the following term: $\Delta m \frac{p_1}{\rho} - \Delta m \frac{p_2}{\rho} + \Delta m g z_1 - \Delta m g z_2 = \frac{1}{2}\Delta m u_2^2 - \frac{1}{2}\Delta m u_1^2$

or $\frac{1}{2}\Delta m u_1^2 + \Delta m g z_1 + \Delta m \frac{p_1}{\rho} = \frac{1}{2}\Delta m u_2^2 + \Delta m g z_2 + \Delta m \frac{p_2}{\rho}$ and simplified (diving by the mass, Δm) to $\frac{1}{2}u_1^2 + g z_1 + \frac{p_1}{\rho} = \frac{1}{2}v_2^2 + g z_2 + \frac{p_2}{\rho}$ giving us $\frac{1}{2}u^2 + gz + \frac{p}{\rho} = K$, where K is a constant. Multiplying by the fluid density (ρ) throughout the equation gives us $\frac{1}{2}\rho u^2 + \rho g z + p = K$ or $q + \rho g h = p_0 + \rho g z = K$ [12], where the dynamic pressure head is given by $q = \frac{1}{2}\rho u^2$, the hydraulic head by $h = z + \frac{p}{\rho g}$ and the total pressure is denoted by $p_0 = p + q$. Finally, the velocity is solved to be $u = \left(2SG\rho g \Delta h\right)^{1/2} / \rho_{air}$. Although the velocity was measured by camera imaging techniques, this velocity (u) is the air velocity in a wind tunnel. The wind tunnel gives drag forces which in turn gives the drag coefficient of the vehicle. By experiment, the model's drag coefficient was found to be 0.40 [13].

Total body weight was fluctuated with varying weights, to cause changes in friction forces thereby keeping drag forces relatively constant. Then numerical analysis techniques were used to converge on the coefficient of rolling resistance, by initially treating the drag coefficient as an unknown, and then as neglecting it altogether due to the low speeds of the speed trap tests. Lastly, drag coefficient of the same car was found experimentally from wind tunnel analysis and was substituted to the simplified equations of motions during the tests.

At coast down, i.e. when the engine is not providing power to the axles any longer, the body travels with the initial momentum and ultimately comes to a stop exclusively due to drag and friction forces slowing the car down, i.e the forces involved are:

$F_{Drag} = \frac{1}{2} C_D \rho_{air} A_{frontal} V^2$ and $F_{Rolling} = C_{rr} W_{car} \overline{V}$ respectively.

Both forces, F_{Drag} and $F_{Rolling}$ are depended on the velocity of the travelling car. Historically, scientists and engineers, used various other methods to quantify the value using a velocity dependent expression and a model that neglected the latter, i.e. it was not adjusted for velocity [14]. These expressions can be said to be $F_{Rolling} = C_{rr} W_{car}$ which can be characterized for a slow rigid (minimum deformation) wheel as $C_{rr} = \left(\frac{z_{depth}}{d_{wheel}} \right)^{1/2}$ with z_{depth} as the depth of wheel sinkage and d_{wheel} (r_{wheel} is wheel radius) as wheel diameter. A length dimension rolling friction coefficient was also introduced as $F_{Rolling} = \frac{W_{car} C_{rr}}{r_{wheel}}$. These simple models however were used before complex expressions were experimentally developed and do not directly correlate to recent data, but simply shows the relationships between the cars weight, the corresponding rolling frictional forces it experiences and the size of its wheels. It mainly leaves out any consideration for the travelling velocity. In effect, the rolling friction coefficient of a metal wheel of the same dimensions as a rubber wheel with equal loading and same rolling friction will give the same rolling resistance value. In this study, velocity was taken into consideration.

3. RESULTS AND DISCUSSION

3.1 Experimental Results

Tables 1 – 4 show velocity, time and acceleration measurements at varied weight conditions. Table 5. shows mean velocity and acceleration data from each of the weighted tests (Tables 1 – 4). Table 6. is the first iteration conducted by a numerical analysis package (Least Square Linear Regression and Optimization Technique) utilizing a random initial guess, while Table 7. is the second and final iteration.

Tables 1-4. Distance, time, velocity and acceleration data

	SC_{ent} (in)	L_1, L_2	SC_{ex} (in)	X_1, X_2	V_{ent} mph	V_{ex} mph	$\overline{V}$ mph	Δt sec	$\frac{\Delta V_0}{\Delta t}$ m/s²
Set 1	0.58	19, 30	0.63	24, 28	10.82	4.26	8.45	0.78	-8.41
Trials 1-4	0.58	14, 26	0.50	29, 33	11.80	3.41	8.30	0.77	-10.85
m_t=2004.7 g	0.58	19, 28	0.75	19, 21	8.85	2.56	9.02	1.03	-6.10
	0.63	20, 30	0.60	23, 28	10.65	5.11	10.87	0.75	-7.43
	0.48	12, 26	0.45	27, 34	11.55	5.42	9.06	0.69	-8.84
Set 2	0.54	12, 25	0.56	23, 28	11.87	4.73	8.20	0.71	-10.08
Trials 1-4	0.68	17, 27	0.60	24, 29	11.62	5.11	8.95	0.70	-9.26
m_t=1912.6 g	0.60	20, 31	0.60	28, 33	11.25	5.11	9.34	0.72	-8.54
	0.63	24, 32	0.71	27, 29	8.52	2.44	8.96	1.07	-5.67
	0.54	18, 28	0.56	24, 30	9.13	5.68	10.06	0.79	-4.34
Set 3	0.47	8, 22	0.31	14, 24	11.19	5.22	8.30	0.72	-8.32
Trials 1-4	0.50	14, 30	0.42	9, 15	13.64	4.26	8.37	0.66	-14.27
m_t=1723.6 g	0.58	11, 24	0.58	12, 18	12.78	5.90	8.18	0.63	-10.94
	0.79	17, 26	0.68	24, 29	12.11	5.81	5.48	0.66	-9.60
	0.56	13, 26	0.42	8, 19	12.31	7.81	7.41	0.58	-7.70
Set 4	0.47	8, 23	0.29	7, 17	11.99	4.92	7.54	0.70	-10.16
Trials 1-4	0.52	14, 28	0.31	7, 15	12.34	4.26	7.60	0.71	-11.41
m_t=1237.6 g	0.38	9, 29	0.21	5, 20	12.78	5.25	5.70	0.65	-11.55
	0.60	7, 22	0.42	11, 20	15.34	6.39	7.88	0.54	-16.54
	0.63	9, 22	0.42	9, 15	13.85	4.26	8.49	0.65	-14.76

Table 5. Overall data from all 4 data sets at varying total weights

Set	m_t gram	W kg	m/s²)	$\overline{V}_{ent}$ mph	$\overline{V}_{ex}$ mph	ΔV_0 mph	m/s	$\overline{\Delta t}$ sec	$\frac{\Delta V_0}{\Delta t}$ m/s²	$\overline{V}$ mph
1	1237.6	12.1		13.3	5.0	-8.2	-3.69	0.649	-5.68	9.14
2	1723.6	16.9		12.4	5.8	-6.6	-2.95	0.649	-4.55	9.10
3	1912.6	18.8		10.5	4.6	-5.9	-2.62	0.799	-3.28	7.55
4	2004.7	19.7		10.7	4.2	-6.6	-2.94	0.805	-3.66	7.44

$\Delta V_0 = \overline{V}_{ex} - \overline{V}_{ent}$, where $\overline{V}_{ex}$ and $\overline{V}_{ent}$ are the mean set velocity readings from weighted test runs, set 1-4. $W = m_t * g$, where m_t is the total vehicle mass and g is the gravitational acceleration constant.

As mentioned before, SC_{ent} and SC_{ex} are scaling factors incorporated in calculation to correctly take the board distance into consideration in the calculation of data in sets 1-4 in Table 5. From the above data, we further quantify results into force components (Table 6. and 7) and solve numerically for C_{rr} and C_D.

Table 6-7. Total forces acting on vehicle model and subsequent iterations

	$F_{Supplied}$ $m_t\left(\frac{\Delta V_0}{\Delta t}\right)$	F_{Drag} $C_{D.}\alpha$	$F_{Rolling}$ $C_{rr.}\beta$	$\Sigma\,(F_{Drag+}$ $F_{Rolling})$ $C_{D.}\alpha + C_{rr.}\beta$	$\Delta\,\lvert F_{Supplied} - \Sigma\, F_{D,\,R}\rvert$ $\lvert m_t\left(\frac{\Delta V_0}{\Delta t}\right) - C_{D.}\alpha -$ $C_{rr.}\beta\rvert$
1st Iteration	-7.02	-5.55	-0.009	-5.56	1.46
	-7.84	-7.70	-0.009	-7.71	0.13
	-6.27	-7.08	-0.006	-7.09	0.82
	-7.33	-7.32	-0.006	-7.33	0.00
2nd Iteration	-7.023	-4.507	-0.026	-4.53	2.49
	-7.843	-6.276	-0.026	-6.30	1.54
	-6.271	-6.965	-0.018	-6.98	0.71
	-7.329	-7.300	-0.017	-7.32	0.01

Since $\sum F = 0$, $F_{Supplied} - F_{Drag} - F_{Rolling}$ at coast down; or $m_t\left(\frac{\Delta V_0}{\Delta t}\right)$ - $\frac{1}{2}\,C_D\rho_{air}A_f\left(V+V_0\right)^2$ - $C_{rr}m_t gV$. Let $\alpha = -\frac{1}{2}\rho_{air}A_{frontal}\left(V+V_0\right)^2$ and $\beta = WV$ where $W = m_t g$

The above two iterations of least square methods yield a coefficient of rolling resistance of 0.1119 and then 0.3712, while the coefficient of aerodynamic drag yields 0.0416 and 0.1165, respectively. Other linear regression techniques such as Huber M, the least absolute deviations and nonparametric regressions can be used but due to the analysis of simple non skewed and non-high tailed data distributions in Tables 6 and 7, Least Squares optimization technique was preferred [15].

This analysis however were conducted assuming the coefficient of drag is a variable or an unknown, and an initial guess was selected to provide a starting point for the iterations, resulting in possibly erroneous end result. The same analysis was conducted by eliminating the drag coefficient, thereby only solving for the rolling friction constant, since at slow speeds, the drag coefficient is effectively negligible. Similarly knowing that the drag coefficient for the model is 0.40, we can treat F_{drag} as a constant, thereby solving for the C_{rr} again as follows.

Table 8. Calculating Coefficient of Rolling Resistance with C_D= 0 and C_D= 0.40

	$F_{Supplied}$	F_{Drag}	$F_{Rolling}$	C_{rr}	$\overline{C_{rr}}$
F_{drag}= 0.0	-7.02	0	49.6	-0.142	-0.117
(C_D =0.0)	-7.84	0	68.81	-0.114	
	-6.27	0	63.31	-0.099	
	-7.33	0	65.44	-0.112	
F_{drag}= α_i*C_D	-7.02	-0.089	49.6	-0.140	-0.115
(C_D =0.40)	-7.84	-0.088	68.81	-0.113	
	-6.27	-0.060	63.31	-0.098	
	-7.33	-0.059	65.44	-0.111	

Knowing that the rolling resistance coefficient for a car, the size of the test model would lie in between the ranges found, assuming drag forces to be negligible (i.e. F_{Drag}~0.0 resulting in a C_{rr} of 0.117, (Table 8.). The coefficient is found experimentally after assuming that the model has a known constant drag coefficient (i.e. $F_{Drag} = -\frac{1}{2} C_D \rho_{air} A_{frontal} \left(V + V_0\right)^2$, where C_D is a constant of value 0.40) resulting in a C_{rr} of 0.115). The average coefficient of rolling resistance for the experiment therefore would be 0.116. The mean C_{rr} can be computed as:

$$\overline{C_{rr}} = M \cdot \left| \frac{f_{rr,C_D \to K} + f_{rr,C_D \to 0}}{2} \right|$$

where K is approaching the value of the coefficient of aerodynamic drag, i.e. less than or greater than C_D ; Hence ($K \neq C_D$). Also, n is the total lines crossed, or more specifically, n is the exit position with $n-1$ the entrance position in the speed trap set up and M is the model-vehicle scale. Moreover,

$$f_{rr,C_D \to K} = \frac{m_t}{2 \cdot \beta \cdot \Delta t} \left[\frac{1}{t_{fps}} \cdot (X_n - X_{n-1} + L_n - L_{n-1}) \right]_{SC_{n,n-1}} - \frac{1}{\beta} \cdot C_D \cdot A_{frontal} \cdot SG \cdot \rho \cdot \Delta h \quad \text{with}$$

the wind tunnel automotive drag force at varying tunnel air velocities of u_0, where $u = \left(2SG\rho g \Delta h\right)^{1/2} / \rho_{air}$ or just

$$f_{rr,C_D \to K} = \frac{m_t}{2 \cdot \beta \cdot \Delta t} \left[\frac{1}{t_{fps}} \cdot (X_n - X_{n-1} + L_n - L_{n-1}) \right]_{SC_{n,n-1}} - \frac{1}{\beta} \cdot C_D \cdot \alpha \,,$$

Where

$$\alpha = -\frac{1}{2} \rho_{air} A_{frontal} \left(V + V_0\right)^2 \text{ and } f_{rr,C_D \to 0} = \frac{m_t}{2 \cdot \beta \cdot \Delta t} \left[\frac{1}{t_{fps}} \cdot (X_n - X_{n-1} + L_n - L_{n-1}) \right]_{SC_{n,n-1}}$$

3.2 Comparative Literature Analysis

The above confirms findings from Ehsani et al. Since a 1:10 scaled model was used for this dynamic testing, the full scale vehicle velocity is given by $\overline{V}_{scaled} = \overline{V}_{full} \times \left(\frac{\rho_{full}}{\rho_{scaled}} \right) \times \left(\frac{D_{full}}{D_{scaled}} \right) \times \left(\frac{\mu_{scaled}}{\mu_{full}} \right)$ meaning, that $\overline{V}_{scale} = 10 \cdot \overline{V}_{full}$, where theoretical C_{rr} for a full scale vehicle is given by $C_{rr,theoretical} = 0.01 \left(1 + \left[\frac{1.609}{100} \right] \times \overline{V}_{full} \right)$ as noted by Ehsani; however, it cannot be automatically used for a scaled model. Conversely,

the velocity cannot be scaled up to that of a full sized vehicle and have the coefficients match between the scaled entities.

Table 9. Comparison of full scale and model vehicle data and error analysis (theoretical model)

$\overline{V}_{scaled}$ **mph**	$\overline{C}_{rr}$	$\overline{C}_{rr,th,sc}$	$\overline{C}_{rr,theory}$	**Error (%)**
9.14	0.014	0.011472	0.11472	18.5
9.10	0.011	0.011465	0.11465	1.14
7.55	0.010	0.011216	0.11216	13.8
7.44	0.011	0.011198	0.11198	0.38

Table 10. Comparison of full scale and model vehicle data and error analysis with patented model (Where $C_{rr,th,sc} = 0.01\left(1+\left[\frac{1.609}{100}\right]\times\overline{V}_{scaled}\right)$ and $\overline{C}_{rr,theory}$ = 10 * $\overline{C}_{rr,th,sc}$ due to scaling, and $\overline{C}_{rr,p}$ =10* $\overline{C}_{rr,p,scaled}$. This scaling is independent of scaling factor incorporated due to Reynolds Number and similitude for the two velocities $\overline{V}$ themselves)

m_t **(kg)**	$\overline{C}_{rr}$	$\overline{C}_{rr,p}$	$\overline{C}_{rr,p,scaled}$	**Error (%)**
1.2376	0.014	0.014934	0.001493	6.67
1.7236	0.011	0.012655	0.001265	15.05
1.9126	0.010	0.012013	0.001201	20.13
2.0047	0.011	0.011734	0.001173	6.67

Here $\overline{C}_{rr}$ represents the average experimental values of the coefficients with and without considering the effects of drag at given speeds $\overline{V}_{scaled}$ (in mph). Knowing that $\overline{C}_{rr,theory}$ is given for full scale vehicles, to scale down to the 1:10 ratio, we multiply the $\overline{C}_{rr,th,sc}$ value by 10 to get data for the scaled model. The coefficient can be greatly changed by tire pressure, speed *u*, loading (curb weight), wheel diameter and gap in data or measuring instruments, which is why most dynamic analysis do not directly correlate to literature data and result in errors [16]. A slight change of the consistency of the ground material (concrete, sandy soil, loose soil, asphalt) changes the coefficient value dramatically [17]. Recent Studies also show that C_{rr} can range from a higher interval of 0.006 to 0.035 [18]. This is a direct confirmation of the present study as the experimental range for the current study falls in this interval; with, however, a high error of 43.416% for the mean values. Other studies concluded that tires have a rolling resistance coefficient C_{rr} of a range from 0.007 to 0.014 [19] (or a 10.47% error in the mean values). Common values for the rolling resistance coefficient of a full sized vehicle travelling on concrete range from 0.010 to 0.015 [20], or a mean of 0.0125. With respect to the current study, this yields a 7.2% error. See also Table 9. The average $C_{rr,th,sc}$ [20] model values and the C_{rr} values of the study share a 2.31% error with each other. Although using the model-to-vehicle scaling ratio can be used to estimate the rolling friction coefficient for the actual vehicle, there are a lot of variables in such real life testing. To best optimize accuracy using this method, the curb weight for both the vehicles would need to be maintained, in addition to both overall exterior scale and tire dimensions. A

standard model known as SAE J1269 was developed by the Society of Automotive Engineers (SAE) to quantify the coefficient in the United States. C_{rr} measured in the study using the Force, Torque and Power methods denote the rolling resistance coefficient being measured as the proportion of energy that is lost to the hysteresis of the material as the tire rolls [21]. The study results of the general coefficient and its comparison to the applied forces at wheels are in agreement with secondary research [22]. Another standard, SAE J2452 provided more accuracy for C_{rr} value over a range of different vehicle loads (weight), tire pressures and vehicle speeds [23]. The model expression for the standard is defined as:

$C_{rr} = P^{\alpha} \times Z^{\beta} \times \left(a + bV + cV^2 \right)$, where P is the tire inflation pressure (in kPa or psi), Z is the applied load for vehicle weight (in N or lbs), V is the vehicle speed (in km/h or mph) and α, β, a, b, c are the constant coefficients for the model (Society of Automotive Engineers 1999). In Europe, rolling resistance is tested using the standard ISO 8767 [24]. The SAE standard is similar to a patented C_{rr} calculated methodology, where the distance time data during the coast down motion is effectively expressed by applying Newton's Second law of motion [25], or $\frac{W}{g}(1+f)\frac{dV}{dt} = D_T + D_R + D_a$, where D_T represent transmission loss, given by $D_T = W(\tau_0 + bV)$ and D_R, D_a represent Rolling friction loss and aerodynamic drag loss respectively denoted by $D_R = W\left(\left[\frac{(nI_w + I_d)g}{WR^2}\right] + kV^2\right)$ and $D_a = C_D \cdot \left(\frac{1}{2}g\right)V^2 \cdot F$. The same expression can be written as $\frac{\delta}{g}\frac{dV}{dt} = a + bV + cV^2$, where $\delta = 1 + f$, $a = \tau_0 + f_0$ and $c = k = \frac{\rho \cdot C_D \cdot F}{2 \cdot g \cdot W}$. To obtain the velocity time data, the expression is integrated to yield $\frac{dS(t)}{dt} = V(t) = \frac{\delta}{gc}\left[B\tan(\tan^{-1}(\frac{h}{B}) + B(T-t)) - h\right]$, where $S(t)$ is the distance travelled by the vehicle from rest till t, T is the time from arbitrary t till stop. Accordingly, $B = \left[\frac{gA}{2\delta}\right]$, $A = \sqrt{4ac - b^2}$ and $h = \left[\frac{gb}{2\delta}\right]$. Similarly, the expression can be further integrated to yield data for distance-time, i.e $S(t) = \frac{\delta}{gc}\left[\ln\frac{\cos\left\{\tan^{-1}\left(\frac{h}{B}\right)\right\}}{\cos\left\{\tan^{-1}\left(\frac{h}{B}\right) + BT\right\}} - ht\right]$, where substituting $t=T$ gives $S(T) = \frac{\delta}{gc}\left[\ln\frac{\cos\left\{\tan^{-1}\left(\frac{h}{B}\right)\right\}}{\cos\left\{\tan^{-1}\left(\frac{h}{B}\right) + BT\right\}} - hT\right]$. Here $S(T)$ denotes the distance travelled from time T till the ultimate rest. The distance time data from the tests can be used in the

expression to yield unknown coefficient values by least square optimization and curve fitting techniques (Numerical Analysis). Using the equation, $-\frac{\delta_0}{g}\frac{dV}{dt} = \tau_0 + bV$, the transmission loss can be effectively neglected. Here $\delta_0 = g\left[\frac{mI_w + I_d}{WR^2}\right]$ is the effective mass of the rotating parts, with *m* being the total number of driving tires (usually 2). Integrating the expressions twice gives $\frac{dS(t)}{dt} = V(t) = \frac{\tau_0}{b}\cdot\left[\mathrm{e}^{(\{T-t\}h_0)-1}\right]$ and $S(t) = \frac{\tau_0}{bh_0}\cdot\left[\mathrm{e}^{T\cdot h_0} - \mathrm{e}^{(T-t)\cdot h_0}\right] - \frac{\tau_0}{b}\cdot t$, where if it is assumed that *T=t*. Then $S(t) = \frac{\tau_0}{b}\cdot\left[\frac{\mathrm{e}^{T\cdot h_0}-1}{h_0} - T\right]$ and neglecting transmission loss again, yields $S(T_i) = \frac{\tau_0}{b}\cdot\left[\frac{\mathrm{e}^{T_i\cdot h_o}(\mathrm{e}^{T_r\cdot h_0}-1)}{h_0} - T_i\right]$, where *I* and *r* refers to the last point on the track to the point next to it (closer to the vehicle) during travel and h_0 and δ_0 can be defined as $h_0 = \frac{gb}{\delta_0}$ and $\delta_0 = \frac{(mI_w - I_d)g}{WR^2}$.Using test data, it can be said that $2\Delta S + \Delta S^* = \frac{\tau_0}{b}\cdot\left[\frac{\mathrm{e}^{T_r\cdot h_0}\{\mathrm{e}^{T_1\cdot h_0}-1\}}{h_0} - T_1\right]$ and $\Delta S + \Delta S^* = \frac{\tau_0}{b}\cdot\left[\frac{\mathrm{e}^{T_r\cdot h_0}\{\mathrm{e}^{T_2\cdot h_0}-1\}}{h_0} - T_2\right]$ and $\Delta S^* = \frac{\tau_0}{b}\cdot\left[\frac{\mathrm{e}^{T_r\cdot h_0}\{\mathrm{e}^{T_3\cdot h_0}-1\}}{h_0} - T_3\right]$, where the three variables τ_0, *b* and T_r can be obtained from the three preceding equations. Let the short distance coast down be $S(T_i) = \frac{\delta}{gc}\left[\ln\frac{\cos\left\{\tan^{-1}\left(\frac{h}{B}\right) + BT_r\right\}}{\cos\left\{\tan^{-1}\left(\frac{h}{B}\right) + B(T_r + T_i)\right\}} - hT_i\right]$,

where $B = \left[\frac{gA}{2\delta}\right]$, $A = \sqrt{4ac - b^2}$ and $h = \left[\frac{gb}{2\delta}\right]$.Or it follows that

$$3\Delta S = \frac{\delta}{gc}\left[\ln\frac{\cos\left\{\tan^{-1}\left(\frac{h}{B}\right)+BT_r\right\}}{\cos\left\{\tan^{-1}\left(\frac{h}{B}\right)+B(T_r+T_1)\right\}}-hT_1\right],$$

$$2\Delta S = \frac{\delta}{gc}\left[\ln\frac{\cos\left\{\tan^{-1}\left(\frac{h}{B}\right)+BT_r\right\}}{\cos\left\{\tan^{-1}\left(\frac{h}{B}\right)+B(T_r+T_2)\right\}}-hT_2\right] \text{ and}$$

$$\Delta S = \frac{\delta}{gc}\left[\ln\frac{\cos\left\{\tan^{-1}\left(\frac{h}{B}\right)+BT_r\right\}}{\cos\left\{\tan^{-1}\left(\frac{h}{B}\right)+B(T_r+T_3)\right\}}-hT_3\right]$$ Due to the behavior of drag and rolling friction, we can now say $3\Delta S = \frac{\delta}{gc}\left[\ln\frac{\cos\left\{\tan^{-1}\left(\frac{h}{B}\right)+BT_r\right\}}{\cos\left\{\tan^{-1}\left(\frac{h}{B}\right)+B(T_r+T_1)\right\}}-hT_1\right]$ and $\Delta S = \frac{\delta}{gc}\left[\ln\frac{\cos\left\{\tan^{-1}\left(\frac{h}{B}\right)+BT_r\right\}}{\cos\left\{\tan^{-1}\left(\frac{h}{B}\right)+B(T_r+T_3)\right\}}-hT_3\right]$ assuming that the tests determine the total resistance of the vehicle in accordance with $\frac{\rho}{g}\cdot\frac{dV}{dt} = a + bV + cV^2$, where ρ is the air density and g is the gravitational constant. Additionally, coefficients *a, b* and *c* refer to rolling and internal transmission resistance and subsequent losses, *b* is transmission loss and *c* is aerodynamic drag and rolling loss. Coefficient *b* can determined from the expression $S(T_i) = \frac{\tau_0}{b}\cdot\left[\frac{e^{T_i\cdot h_o}(e^{T_r\cdot h_0}-1)}{h_0}-T_i\right]$ while coefficients *a* and *c* are determined from $S(T_i) = \frac{\delta}{gc}\left[\ln\frac{\cos\left\{\tan^{-1}\left(\frac{h}{B}\right)+BT_r\right\}}{\cos\left\{\tan^{-1}\left(\frac{h}{B}\right)+B(T_r+T_i)\right\}}-hT_i\right]$, where T_i is the time taken for the vehicle to travel to the i^{th} position in the speed trap. Again, $h = \left[\frac{gb}{2\delta}\right]$, $h_0 = \left[\frac{gb}{\delta_0}\right]$, $B = \left[\frac{gA}{2\delta}\right]$ and $A = \sqrt{4ac-b^2}$. Recalling that, $\delta = 1+f$, $f = \frac{(nI_w + I_d)g}{WR^2}$,

$\delta_0 = \frac{(MI_w + I_d)g}{WR^2}$, $a = \tau_0 + f_0$ and finally $k = \frac{\rho \cdot C_D \cdot F}{2 \cdot g \cdot W}$. However, here in this study, we multiply the coefficient value with the scales since this test is conducted on a trap regardless of size, unlike the model by Ehsani et al 2009. This results in higher error due to the precision of the tests, and negligence of the transmission losses. Still, the current study data on average comes within 0.005 of the patented results as shown in Table 10. The knowledge of this data has various applications in performance analysis and design of locomotives, as lower C_{rr} tires could save 1.5–4.5% of all gasoline consumption [26]. Even correcting wheel sinkage during maneuvering through sandy terrains [27] or misalignment correction by wheels aboard microsatellites during orbital maintenance [28] can be done. Better designs have led to reduced coefficient values at the wheels in cars (around 0.0025) [29]. In normal passenger vehicles, energy is wasted by rolling frictions effects on the highways in which sound and heat is generated and given off to the surroundings as a by-product by the tires [30].

4. CONCLUSION

Although industrial machines have been designed so as to have the ability to quantify the rolling friction coefficient of a tire, such equipment is usually not within the reach of most designers or scientists. The presented model is a small scaled and low cost technique that not only gives the scaled coefficient value with an acceptable degree of accuracy, but can be used to extrapolate the value to a full scaled car as long as weighted and scaled proportions, i.e. vehicle curb weight and tire size are the same.

ACKNOWLEDGEMENTS

This study by the Sustainable Automotive Energy Infrastructure (KU Ecohawks, 2008-2009) Initiative at the University of Kansas was partially supported by the KU Transportation Research Institute and relied on the guidance from Dr. Christopher C. Depcik, and the assistance of Jason A. Carter at the Department of Mechanical Engineering.

COMPETING INTERESTS

Author has declared that no competing interests exist.

REFERENCES

1. Hibbeler RC. Engineering mechanics. Pearson Education; 2002.
2. Ehsani, M, Yimin G, Ali E. Modern electric, hybrid electric, and fuel cell vehicles: fundamentals, theory, and design. CRC; 2009.
3. Hussain SA, Tan HT, Idris A. Numerical Studies of Fluid Flow Across a Cosmo Ball by Using CFD. Journal of Applied Sciences (Faisalabad). 2010;10(24):3384-3387.
4. Rimy MM, Faieza AA. Simulation of Car Bumper Material using Finite Element Analysis. Journal of Software Engineering. 2010;4(3):257-264.
5. Wang, ZP, Qian XJ. Simulation of Rolling Resistance of Tire Based on ANSYS. Advanced Materials Research. 2011;156:592-595.
6. Petrushov VA. Improvement in vehicle aerodynamic drag and rolling resistance determination from coast-down tests. Proceedings of the Institution of Mechanical Engineers, Part D: Journal of Automobile Engineering. 1998;212(5):369-380.

7. Buckingham, E. On physically similar systems; illustrations of the use of dimensional equations. Physical Review. 1914;4(4):345-376.
8. Sunny, SA. Effect of turbulence in modeling the reduction of local drag forces in a computational automotive model. International Journal of Energy and Environment. 2011;2(6):1079-1100.
9. Bernoulli D, Bernoulli J. Hydrodynamics. Translated from the Latin by Thomas Carmody and Helmut Kobus; 1968.
10. Tipler PA, Gene M. Physics for scientists and engineers. Vol. 1. Wh Freeman; 2007.
11. Feynman RP, Leighton RB, Sands M, Treiman SB. The Feynman lectures on physics. Physics Today. 1964;17:45.
12. Oertel, H. Prandtl's essentials of fluid mechanics. Vol. 158. Springer Verlag; 2004.
13. Sunny SA. Study of the Wind Tunnel Effect on the Drag Coefficient (C_D) of a Scaled Static Vehicle Model Compared to a Full Scale Computational Fluid Dynamic Model. Asian Journal of Scientific Research. 2011;(4):236-245.
14. Peck WG. Elements of mechanics: for the use of colleges, academies, and high schools. AS Barnes; 1872.
15. Mohebbi M, Nourijelyani K. Zeraati H. A Simulation Study on Robust Alternatives of Least Squares Regression. Journal of Applied Sciences. 2007;7(22):3469-3476.
16. Qinynian W. A Calculation Method of the Sinkage and Rolling Resistance of a Rigid Wheel with Multi-Pass on Loose soil. Journal of Jilin University of Technology (Natural Science Edition). 1987;3:011.
17. Dai J, Wang J, Gao W. Application of Bench-based Rolling Resistance of Tires Model. Transactions of the Chinese Society of Agricultural Machinery. 2003;011.
18. Schmidt B, Ullidtz P. Special Report Danish Road Directorate and Dynatest. NCC Green Road: Energy savings in road transport as a function of the functional and structural properties of roads: A Technical Report. Accessed 18 July 2011. Available: http://trid.trb.org/view.aspx?id=1151232.
19. National Research Council. TRB Committee for the National Tire Efficiency Study. Tires and Passenger Vehicle Fuel Economy: Informing Consumers, Improving Performance. Vol. 286. Transportation Research Board National Research; 2006. Accessed 7 June 2011. Available: http://onlinepubs.trb.org/onlinepubs/sr/sr286.pdf.
20. Gillespie TD. Fundamentals of Vehicle Dynamics. Warrendale, PA: Society of Automotive Engineers. 1992;195-236.
21. Society of Automotive Engineers. SAE J1269: Rolling Resistance Measurement Procedure for Passenger Car, Light Truck, and Highway Truck and Bus Tires. SAE International Publications. 2006. Accessed 22 November 2010. Available: http://standards.sae.org/j1269_200609/.
22. Lenard, JG. Primer on flat rolling. Elsevier Science Limited; 2007.
23. Society of Automotive Engineers. SAE J2452: Stepwise Coast down Methodology for Measuring Tire Rolling Resistance. SAE International Publications; 1999. Accessed 5 May 2010. Available: http://standards.sae.org/j2452_199906/.
24. International Organization for Standardization, ISO 8767: Passenger car tyres - Methods of Measuring Rolling Resistance. TC 31/SC 3. ICS: 83.160.10. (Revised: ISO 18164:2005) 1992. Accessed 22 November 2010. Available: http://www.iso.org/iso/catalogue_detail.htm?csnumber=16179.
25. Hur N, Ahn L, Petrushov VA. Method for measuring vehicle motion resistances using short distance coast-down test based on the distance-time data. U.S. Patent 5,686,651, issued November 11; 1997.
26. Calwell, C. California State Fuel-Efficient Tire Report, Volume II, California Energy Commission. 2003. Accessed 8 May 2010. Available: http://www.energy.ca.gov/reports/2003-01-31_600-03-001CRVOL2.PDF.

27. Liu, J, Gao H, Deng Z. Effect of straight grousers parameters on motion performance of small rigid wheel on loose sand. Information Technology Journal. 2008;7(8):1125-1132.
28. Mohammed, AM, Benyettou M, Chouraqui S, Hashida Y, Sweeting MN. Wheel Attitude Cancellation Thruster Torque of LEO Microsatellite during Orbital Maintenance. Journal of Applied Sciences. 2006;6:2245-2250.
29. Roche DM, Schinckel AER, Storey JWV, Humphris CP, Guelden MR. Speed of Light: The 1996 World Solar Challenge. Photovoltaics Special Research Centre; 1997.
30. Hogan CM. Analysis of highway noise. Water, Air, & Soil Pollution. 1973;2(3):387-392.

Peer-review history:
The peer review history for this paper can be accessed here:
http://www.sciencedomain.org/review-history.php?iid=210&id=5&aid=1277